JOURNAL OF VIROLOGY, June 1997, p. 4626–4637 Vol. 71, No. 6
0022-538X/97/$04.00+0

Long-Term Gene Delivery into the Livers of Immunocompetent Mice with E1/E4-Defective Adenoviruses

JEAN-FRANCOIS DEDIEU,[1] EMMANUELLE VIGNE,[1] CHRISTOPHE TORRENT,[1] CAROLE JULLIEN,[1] IRÈNE MAHFOUZ,[1] JEAN-MICHEL CAILLAUD,[2] NATHALIE AUBAILLY,[3] CÉCILE ORSINI,[1] JEAN-MARC GUILLAUME,[4] PAULE OPOLON,[1] PIA DELAÈRE,[2] MICHEL PERRICAUDET,[1] AND PATRICE YEH[1]*

CNRS URA 1301/Rhône-Poulenc Rorer Gencell, Laboratoire de Génétique des Virus Oncogènes, Institut Gustave Roussy, 94805 Villejuif Cedex,[1] Molecular Histopathology Department, Rhône-Poulenc Rorer Gencell, CRVA, 94140 Alfortville,[2] and Cardiovascular Department[3] and Cellular and Viral Production Department,[4] Rhône-Poulenc Rorer Gencell, CRVA, 94403 Vitry-sur-Seine, France

Received 13 December 1996/Accepted 27 February 1997

We have compared the in vitro and in vivo behaviors of a set of isogenic E1- and E1/E4-defective adenoviruses expressing the *lacZ* gene of *Escherichia coli* from the Rous sarcoma virus long terminal repeat. Infection of tumor-derived established cell lines of human origin with the doubly defective adenoviruses resulted in (i) a lower replication of the viral backbone that correlated with reduced levels of E2A-specific RNA and protein, (ii) a significant shutoff of late gene and protein expression, and (iii) no apparent virus-induced cytotoxicity. Independently of the extent of the deletion, the additional inactivation of E4 from the viral backbone therefore drastically disabled the virus in vitro, with no apparent effect on transgene expression. A *lacZ*-transgenic model was used to compare the different recombinant adenoviruses in the livers of C57BL/6 mice. The immune response to the virally encoded β-galactosidase was minimal in this model, as infusion of the E1-defective adenovirus resulted in a time course of transgene expression that mimicked that in immunodeficient (*nu*/*nu*) mice, with very little inflammation and necrosis in the liver. Administration of a doubly defective adenovirus to the transgenic animals led to long-term extrachromosomal persistence of viral DNA in the liver, with no detectable methylation of CpG dinucleotides. However, transient transgene expression was observed independently of the extent of the E4 deletion, suggesting that the choice of the promoter may be critical to maintain transgene expression from these attenuated adenovirus vectors.

Wild-type human serotype 2 (Ad2) or serotype 5 (Ad5) adenoviruses naturally infect resting cells (e.g., epithelial cells), in which they induce a lytic productive cycle. Completion of the infectious cycle is primarily dependent on the expression of a set of viral regulatory proteins encoded by early transcription units, including early regions 1 (E1A and E1B) and 4 (E4), which subvert endogenous regulation mechanisms that are crucial for cell viability, viral DNA replication, and virus productivity. For example, E1A and E1B encode a class of oncogenic proteins that drive a quiescent cell into the S phase of the cell cycle (E1A), while escaping apoptosis (E1B), in particular through a coordinate targeting of the RB and p53 proteins (for a recent review, see reference 45). E4 is another region that is essential for virus growth, as a result of its pleiotropic involvement in viral gene expression, DNA replication, and particle assembly (16, 23). Located at the right end of the virus genome (Fig. 1), E4 encodes regulatory proteins that act throughout the infectious cycle. This is the case for the E4orf6/7 protein, which associates with endogenous DP-1/E2F transcription factors (2, 15, 24, 37), transforming them into E2A-specific transactivators during the early phase of infection, thereby illustrating the pleiotropic involvement of E4 in the control of virus DNA replication (54, 55) and transcription (8, 62). E4 is also required for the emergence and/or cytoplasmic accumulation of spliced mRNAs derived from the late primary transcript that encode most of the virion structural proteins (5, 23, 25). These posttranscriptional modifications are dependent upon an essential function shared by the E4orf3 and E4orf6 proteins (27), which somehow regulates the extensive maturation of this 28-kb-long RNA molecule and/or the subsequent nuclear export of its corresponding mRNAs. Accordingly, in vitro data suggest that both Ad5 E4 proteins, directly or indirectly, modulate the splicing modalities within a human cell, including exon skipping and the recognition of distal splice acceptor sites (36). The E4orf6 protein exhibits additional functions through its interaction with the E1B 55-kDa protein (20), regulating export of viral and cellular mRNAs from the nucleus (1, 40, 43). The E4orf6 protein has also been reported to interact with the C-terminal regulatory domain of the p53 tumor suppressor, inhibiting p53-dependent transactivation and apoptosis (13, 34). Another E4 protein, the E4orf4 protein, apparently associates with endogeneous phosphatase 2A, modulating the function of viral (e.g., E1A) and cellular transcription factors (4, 28, 35).

Drastically attenuated versions of Ad2 and Ad5 have been engineered following deletion of the E1A and E1B transcription units. As a consequence, these deletants do not propagate in most human cells except within artificial (packaging) cell lines that provide in *trans* the missing regulatory functions. Since 1993, E1-deleted recombinant viruses that contain a transgene expression cassette inserted in place of the E1 region have been evaluated in phase I clinical trials that target proliferative (e.g., cancer) or recessive deficiency (e.g., cystic fibrosis) disorders. Most (i.e., 80%) of the 36-kb viral genome is retained within these vectors, and the sole deletion of E1 cannot completely abrogate viral gene expression. For example, early (the 72-kDa E2A-encoded product) and late (the

* Corresponding author. Mailing address: Laboratoire de génétique des virus oncogènes, CNRS/URA 1301, Institut Gustave Roussy, 39 rue Camille Desmoulins, 94805 Villejuif Cedex, France. Phone: (33) 1 42 11 50 89. Fax: (33) 1 42 11 52 46. E-mail: pyeh@igr.fr.

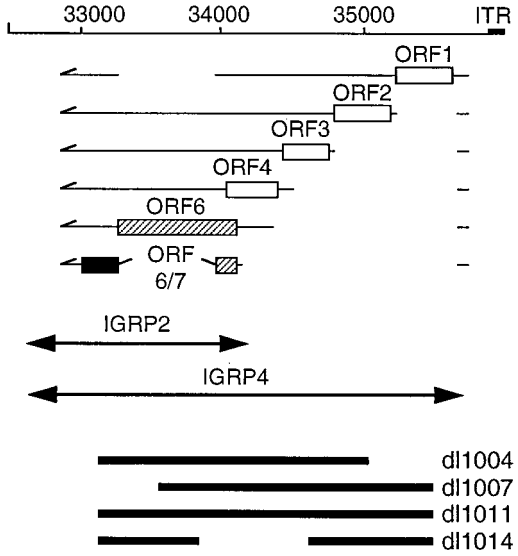

FIG. 1. Mapping of the different E4 deletion mutations used in this study. The physical map of the right end of the Ad5 genome is shown at the top. Numbers refer to the nucleotide positions, starting from the left end of the genome. The positions of the main mRNAs (thin arrows) encoding E4orf1, -orf2, -orf3, -orf4, -orf6, and -orf6/7 (boxes) are from reference 12. H5dl1004, H5dl1007, H5dl1011, and H5dl1014 (black bars) are E4 deletion mutants that were used to construct the E1/E4-defective viruses (see Materials and Methods). Double-headed arrows delineate the E4 sequences integrated in the genome of the (E1+E4)-transcomplementing cell lines IGRP2 and IGRP4. ITR, right inverted terminal repeat.

L3-encoded hexon and the L5-encoded fiber) proteins have been detected following administration of E1-deleted viruses in the liver (59), brain (7), lung (14), and muscle (10) tissues of permissive (cotton rat) and nonpermissive (e.g., murine) species. It has been proposed that de novo in vivo synthesis of viral proteins within the transduced cells elicits their major histocompatibility complex class I-restricted destruction by activated cytotoxic effectors (57). The immune response to the virally infected cells accounts, at least in part, for the progressive loss of transgene expression observed following administration of recombinant adenoviruses to immunocompetent hosts (49, 58). In view of these limitations, deletions that inactivate additional nondispensable regulatory genes have been incorporated within the backbone as recently described for the E2A and E4 genes (18, 21, 30, 53, 60). Here we have compared the in vitro and in vivo behaviors of a set of isogenic E1- and E1/E4-defective adenoviruses with different E4 coding potentials.

MATERIALS AND METHODS

Cell lines. 293 is a human embryonic kidney cell line transformed by the E1A and E1B genes of Ad5 (22). Hep3B is a human hepatocarcinoma cell line characterized by an integrated copy of the hepatitis B virus genome. Both cell lines were obtained from the European Collection of Animal Cell Cultures (Salisbury, United Kingdom). They were cultivated at 37°C in 5% CO_2 in minimum Eagle's medium (293 cells) or Dulbecco's modified Eagle medium (Hep3B cells) supplemented with 10% heat-inactivated fetal calf serum and nonessential amino acids. W162 is an E4-transcomplementing cell line of monkey origin permissive for $E1^+E4^-$ human adenoviruses (56). IGRP2 is an E1/E4-transcomplementing cell line that has been derived from 293. It was obtained following transformation of 293 cells with the plasmid pORF6Gen (60), in which the distal (ORF6+ORF7) moiety of Ad5 E4 is under control of the murine mammary tumor virus long terminal repeat (LTR). IGRP4 is similar to IGRP2 except that 293 cells were transfected with plasmid pE4Gen. This plasmid is identical to pORF6Gen except that it contains the entire Ad5 E4 locus (Ad5 nucleotides [nt] 32490 to 35576 [the numbering refers to the sequence under GenBank accession no. M73260]). IGRP2 and IGRP4 cells were cultivated like 293 cells except that 300 μg of Geneticin (Sigma) per ml was added to the culture medium.

Recombinant adenoviruses. AdRSVβGal (48) is an E1-defective virus that expresses a nucleus-targeted β-galactosidase from the Rous sarcoma virus (RSV) LTR. In addition to a deletion of E1 (Ad5 nt 454 to 3328), AdRSVβGal exhibits a large deletion within E3 (Ad5 nt 28592 to 30470). AdE3+βGal is identical to AdRSVβGal except that it contains a complete E3 locus. It was constructed in 293 cells by homologous recombination between the genome of AdβGal/dl1011 (see below) and a plasmid containing the 3.15-kb right-end fragment of the Ad5 genome.

The construction of AdβGal/dl1014 has been previously detailed (60). AdβGal/dl1004, AdβGal/dl1007, and AdβGal/dl1011 were constructed in IGRP4 cells by combining the E1 deletion of AdRSVβGal with the E4 deletion of viruses H5dl1004, H5dl1007, and H5dl1011, respectively (5). Viruses AdβGal/dl1004 and AdβGal/dl1007 were constructed by IGRP4 cells by cotransfection of an *Ase*I-restricted AdRSVβGal genome with H5dl1004 or H5dl1007 *Nsi*I-restricted DNA, respectively. AdβGal/dl1011 was constructed by cotransfecting IGRP4 cells with linearized plasmid pRSVβGal (48) and *Cla*I-restricted H5dl1011 viral DNA. IGRP4 cells were transfected with 5 μg of each partner DNA by the calcium phosphate technique (AdβGal/dl1011) or with the Transfectam Reagent kit (Promega) (AdβGal/dl1004 and AdβGal/dl1007) and allowed to incubate in the presence of 1 μM dexamethasone. Viral progeny was progressively amplified on IGRP4 cells supplemented with dexamethasone prior to plaque purification onto IGRP2 cell monolayers as described previously (60). β-Galactosidase- expressing plaques were randomly picked and amplified on IGRP2 cells, and low-molecular-weight DNA was extracted (26). Recombinant viruses with the expected restriction patterns were subjected to at least another round of plaque purification on IGRP2 cell monolayers and their clonality was assessed by Southern analyses and/or PCR amplification as described previously (60).

Viral stock preparation. Viral stocks of AdβGal/dl1004, AdβGal/dl1007, AdβGal/dl1011, and AdβGal/dl1014 were prepared from viral particles purified from the culture medium of infected IGRP2 cells. Briefly, IGRP2 cells were infected at a multiplicity of infection (MOI) of 3 *lacZ* transduction units (TDU)/cell (see below), and infection was allowed to proceed until complete detachment of the cell monolayer (i.e., 8 to 12 days postinfection [p.i.]). The culture medium was then harvested, clarified by depth filtration, and concentrated by ultrafiltration. Viruses were subsequently purified by step and isopycnic CsCl ultracentrifugations, desalted on PD10 columns (Pharmacia), and eluted in phosphate-buffered saline (PBS), before being aliquoted and stored at −70°C in PBS–10% glycerol. Viral stocks of AdRSVβGal and AdE3+βGal were prepared from infected 293 cells as described above or from intracellular lysates by standard procedures (48).

All viral stocks were titrated on W162 monolayers as TDU, a unit that corresponds to the number of β-galactosidase-positive cells counted after 5-bromo-4-chloro-3-indolyl-β-D-galactopyranoside (X-Gal) staining at 48 h p.i. (60). W162 cells were chosen as indicator cells for titration essentially because there is no endogeneous β-galactosidase background activity in these cells. Viral stocks with similar titers were recovered for all viruses used in this study. After the purification process, this translated into a productivity that ranged from 15 (AdβGal/dl1011) to 60 (AdβGal/dl1014) TDU/cell, compared to 100 TDU/cell for AdE3+βGal. All viral stocks were tested for the presence of replication-competent adenoviruses by using a quantitative assay that detects one replication-competent adenovirus within 10^8 TDU (52). Stocks of AdE3+βGal were negative for doses of 10^7 TDU, and all stocks of the doubly E1/E4-defective viruses were negative for the tested doses (ranging from 2×10^8 to 5.4×10^8 TDU).

Isolation of viral DNA for slot blot and Southern analyses. Hep3B cells grown in six-well dishes were infected at an MOI of 20 TDU/cell, and low-molecular-weight DNA (26) was prepared at different times p.i. Infection controls were systematically included in parallel experiments by counting the number of X-Gal-positive cells at 48 h p.i. Also, a given number of TDU translated into identical amounts of intracellular virus DNA 6 h after infection with any of the E1- or E1/E4-defective recombinant viruses (this report). Undiluted (one-fifth of the preparation) and diluted (10-fold serial dilutions) samples were denatured and applied under vacuum to positively charged polyamine membranes (Nytran-plus; Schleicher & Schuell) by using a Minifold I slot blot apparatus according to the instructions of the manufacturer (Schleicher & Schuell). The membranes were prehybridized for 1 h at 65°C in 0.25 M NaH_2PO_4–0.25 M Na_2HPO_4–7% sodium dodecyl sulfate (SDS). Virus-specific DNA was detected following hybridization of the membrane in the same buffer overnight at 65°C with an Ad5 fragment (pIX and IVa2 regions, nt 3494 to 6314) that was labelled with [α-^{32}P]dCTP by the random primer extension method (Megaprime kit; Amersham). The membranes were washed four times for 5 min each at room temperature in 2× SSC (1× SSC is 0.15 M NaCl plus 0.015 M sodium citrate)–0.1% SDS and then for 10 min at 65°C in 1× SSC–0.1% SDS and twice at 65°C for 10 min in 0.1× SSC–0.1% SDS. Dried membranes were exposed to Fuji RX films with intensifying screens (Hyperscreen; Amersham). For Southern analyses, samples corresponding to one-fifth of the DNA preparations were digested with *Nde*I and run on a 0.8% agarose gel. The fragments were transferred to Nytran-plus membranes and hybridized to an [α-^{32}P]dCTP-radiolabelled probe corresponding to the *Hin*dIII-restricted AdRSVβGal genome. Densitometric analyses were carried out on a Fujix Bas 1000 Bio Imaging Analyser with the MacBas version 2.2 image analysis program (Fuji).

RNA isolation and Northern analyses. Subconfluent Hep3B cell monolayers were infected in 100-mm-diameter petri dishes at an MOI of 20 TDU/cell, and poly(A)$^+$ RNAs were extracted at different times p.i. Again, infection controls were systematically included by counting the number of cells that scored positive following X-Gal staining. Also, to ensure maximum homogeneity among the RNA samples, all RNA preparations to be compared were carried out in parallel. Total cellular RNA was prepared from uninfected and infected cells by phenol extraction at low pH as described previously (47). Poly(A)$^+$ RNAs were isolated by using oligo(dT) columns according to the instructions of the supplier (Life Technologies). One to 2.5 μg of poly(A)$^+$ RNA was denatured in formamide and formaldehyde and electrophoresed in 1× MOPS (morpholinepropanesulfonic acid) buffer through 1% agarose–0.66 M formaldehyde gels as described previously (17). They were capillary blotted to a nylon membrane (Hybond-N; Amersham) for 8 h and baked for 2 h at 80°C. [α-^{32}P]CTP-labelled antisense RNA probes specific for E2A, L3, and L5 transcripts were synthesized by in vitro transcription of appropriate Ad5 inserts cloned into the pBluescript phagemid (Stratagene) or pGEM vectors (Promega). The E2A antisense probe encompasses Ad5 nt 21562 to 23914 (the main body of E2A mRNAs is located between nt 22375 and 24041). The L3 antisense probe encompasses Ad5 nt 18319 to 21567 and thus hybridized to the pVI and hexon mRNAs, as their main bodies extend from nt 18002 to 22396 and nt 18806 to 22396, respectively. The L5 antisense probe encompasses Ad5 nt 31509 to 33594 (the main body of the L5 [encoding fiber] mRNA extends from nt 31042 to 32807). An actin-specific probe was systematically included as a loading and transfer control. It was prepared from a 1.5-kb mouse β-actin cDNA insert (32) cloned into pBluescript. In vitro transcription reactions, prehybridization, hybridization, and washing of the membranes were carried out as recommended by the supplier (Promega). Filters were exposed to Fuji RX films with intensifying screens (Hyperscreen; Amersham).

Immunoprecipitation of adenovirus hexon protein. Subconfluent Hep3B cells grown in 35-mm-diameter petri dishes were mock infected or infected with AdE3+βGal or AdβGal/dl1007 at an MOI of 20 TDU/cell. At various times p.i., cells were washed twice in PBS and labelled for 24 h in 90% methionine-free minimal essential medium–10% minimal essential medium containing 100 μCi/of [^{35}S]-methionine (1 Ci/μmol; New England Nuclear) per ml. The cells were then washed twice in PBS and lysed in radioimmunoprecipitation assay buffer containing aprotinin and phenylmethylsulfonyl fluoride. Equal amounts, as assessed by trichloroacetic acid-precipitable radioactivity, were subjected to immunoprecipitation with 1:10-diluted antihexon antibody (AB 1056; Chemicon) and electrophoresed on SDS–6% polyacrylamide gels. The gels were subjected to fluorography (Amplify; Amersham), dried, and exposed to films with intensifying screens.

Quantification of β-galactosidase activity. Triplicates of subconfluent monolayers of Hep3B cells grown in six-well dishes were infected at an MOI of 20 TDU/cell and allowed to incubate in the absence or presence of cytosine-β-D-arabinofuranoside (araC). araC was added to a final concentration of 50 μg/ml at the time of infection and every 24 h. Cells were harvested by trypsinization, washed twice in PBS, resuspended in lysis buffer (100 mM potassium phosphate [pH 7.8], 1 mM dithiothreitol), and subjected to six cycles of freezing and thawing. Cell debris were removed by centrifugation, and β-galactosidase activity in the supernatant was measured by a chemiluminescence assay (Clontech, Palo Alto, Calif.). Light emission was recorded as a 5-s integral with a Lumat LB9501 luminometer (Berthold, Bad Wildbad, Germany). The protein concentration in the cellular extract was determined with the Bio-Rad protein assay. Viral DNA accumulation was monitored on control wells as described above.

Mice. C57BL/6 mice (*H-2^b*) were obtained from the IFFA Credo (Lyon, France). C57BL/6 *lacZ*-transgenic mice (TG mice) contain the *lacZ* gene under the control of the 5′ regulatory sequence of the β_2-microglobulin gene (9). They were obtained from the Centre de Développement des Techniques Avancées pour l'Experimentation Animale (Orleans, France) following at least 10 consecutive backcrosses with C57BL/6 mice. C57BL/6 immunodeficient mice (C57BL/6 *nu* mice) were obtained from Bomholtgard Ltd. (Ry, Denmark). They were obtained following four backcrosses of *nu*/*nu* mice onto a C57BL/6 genetic background. Adenovirus-mediated gene transfer to the liver was carried out after tail vein injection of 2.5×10^9 to 5.1×10^9 TDU of virus in 200 μl of PBS–10% glycerol. All animal experiments were done in accordance with guidelines from the French Council of Animal Care and Testing.

Histological analyses. Liver samples were fixed in 4% paraformaldehyde for 3 h at 4°C. For morphometric analysis of *lacZ* expression, fixed liver sections were rinsed in PBS, permeabilized with 0.01% (wt/vol) sodium deoxycholate–0.2% (vol/vol) Nonidet P-40 in PBS-$MgCl_2$, and incubated with 3 mM $K_4Fe(CN)$6–3 mM $K_3Fe(CN)_6$–X-Gal in PBS for 4 h at 37°C. Data were quantified by analyzing 10 sections of each infected liver, representing a total of approximately 1,000 hepatocytes. A scoring system for grading virus-induced hepatic inflammation and necrosis from 5-μm paraffin sections stained with hematoxylin and eosin was developed. Liver sections from noninfected animals were graded 0. Inflammation was graded 1 and referred to as minimal when it was characterized by an increased number of intravascular hematopoietic cells competent in immunity and/or inflammation, i.e., lymphocytes and rare neutrophil granulocytes. In grade 2, inflammation was characterized as mild: it was associated with the presence of few small intraparenchymatous lymphocyte foci (typically fewer than 10 per field at a magnification of ×200). Many more (typically 10 to 60 per field at a magnification of ×200) small foci were detected in grade 3 (marked inflammation). The foci were numerous and much larger in grade 4, and they contained numerous plasma cells. Grade 4 refers to inflammation characterized as severe, and it was observed only in the livers of nontransgenic animals infused with the E1-deleted recombinant virus (see Results). Necrosis was referred to as minimal (grade 1) when rare necrotic cells were apparent at the vicinity of the inflammatory foci. Necrosis was characterized as moderate (grade 2) when a few necrotic cells were apparent throughout the liver (i.e., even at sites distant from the inflammatory foci). Occurrence of multicellular necrotic foci indicated a marked necrosis (grade 3). Grade 4 indicated the presence of large patches of necrotic tissues (severe necrosis). With this scoring system, independent examinations of a given slide led to identical results.

Extraction of DNA from liver extracts for slot blot and Southern analyses. Liver fragments were frozen in liquid nitrogen, minced, and incubated overnight in SDS-proteinase K buffer. DNA was prepared following one phenol, two phenol-chloroform, and two chloroform extractions prior to ethanol precipitation and resuspension in water-RNase A (5 μg/ml). For Southern analyses, 20 μg of DNA was digested with *Sal*I or *Not*I prior to electrophoresis in a 0.7% agarose gel run in Tris-acetate-EDTA. The gel was blotted in 0.4 N NaOH onto a Hybond-N+ nylon membrane (Amersham Life Sciences) for 18 h. The filter was washed briefly in 2× SSC and baked at 80°C for 2 h. The membrane was prehybridized for 1 h at 65°C in 5× SSC–5× Denhardt's solution–0.5% SDS–100 μg of salmon sperm DNA per ml, followed by overnight hybridization at 65°C in the same buffer. It was then washed twice at room temperature in 2× SSC–0.1% SDS for 10 min, once in 1× SSC–0.1% SDS at 65°C for 15 min, and twice in 0.1× SSC–0.1% SDS for 10 min, prior to exposure to Fuji RX film at −80°C with an intensifying screen. The probe corresponded to AdRSVβGal *Not*I-digested DNA that was randomly labelled with [α-^{32}P]dCTP. For slot blot analyses, 10 μg of DNA was heated in 0.4 M NaOH–2.2 mM EDTA at 95°C for 2 min and transferred to a Hybond-N+ nylon membrane. DNA was fixed by baking the membrane at 80°C for 2 h. Hybridization was carried out as described above. A second hybridization with a single-copy murine gene consisting of a 1.5-kb *Eco*RI-*Xho*I fragment from the mouse β-actin cDNA (Stratagene) was used as a loading control for standardization. Membranes were exposed to Fuji Imaging Plates (type BAS-IIIS) and analyzed with a Fujix Bas 1000 phosphorimager with the MacBAS version 2.2 program (Fuji Photo Film Co.). In a given quantification experiment, variability was within a 15% range.

RESULTS

Virus construction and titration. Five recombinant adenoviruses were constructed and used in this study (see Materials and Methods). AdE3+βGal is an E1-defective recombinant adenovirus, while AdβGal/dl1004, AdβGal/dl1007, AdβGal/dl1011, and AdβGal/dl1014 exhibit an additional deletion in the E4 locus that renders them doubly defective for growth. All of the recombinant adenoviruses exhibit a complete E3 locus, carry the same β-galactosidase expression cassette inserted in place of E1 (48), and are strictly identical except for the status of their E4 regulatory locus (5). DNA sequencing confirmed that deletions extended from position 33094 to 35052 (*dl*1004), 33467 to 35355 (*dl*1007), and 33094 to 35355 (*dl*1011). The deletion of AdβGal/dl1014 has been assessed previously (60). Accordingly, AdβGal/dl1004 (ORF1+) and AdβGal/dl1014 (ORF4+) retain the potential to express the E4orf1 and E4orf4 proteins, respectively, from the E1A-responsive E4 promoter. In contrast, AdβGal/dl1007 and AdβGal/dl1011 exhibit larger deletions which abrogate synthesis of all E4-encoded gene products (Fig. 1).

Concentrated purified stocks of the E1- and E1/E4-defective recombinant viruses were prepared, and the clonality of each virus was demonstrated by restriction analysis, Southern blotting, and/or PCR amplification of the viral DNA (data not shown). Because comparison of the titers of E1- and E1/E4-defective viruses on the basis of PFU is only marginally relevant due to the use of indicator cell lines with different plaquing efficiencies, titers were expressed as TDU within W162 cells. The E4-positive status of the W162 indicator cell line does not introduce any bias when E4-competent or E4-defective viruses are titrated, because transduction titers were identical following infection of its E4-defective parental cell line (Vero). The titers of the AdRSVβGal or AdE3+βGal virus expressed as PFU on 293-derived monolayers are roughly twice those determined as TDU in W162 cells.

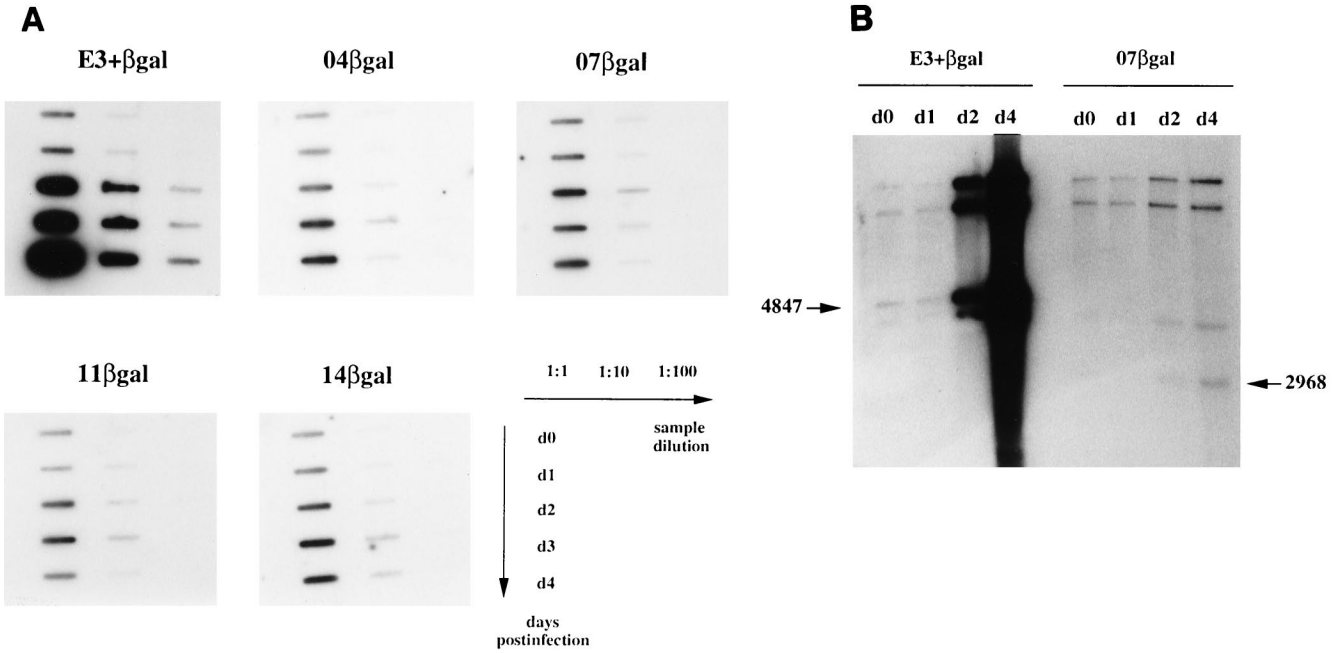

FIG. 2. Comparative analysis of viral DNA accumulation in Hep3B cells. Cells were infected at an MOI of 20 TDU/cell with the indicated virus (E3+βgal, 04βgal, 07βgal, 11βgal, and 14βgal refer to viruses AdE3+βGal, AdβGal/dl1004, AdβGal/dl1007, AdβGal/dl1011, and AdβGal/dl1014, respectively). Low-molecular-weight DNA was prepared at 6 h p.i. (day 0) and every 24 h (days 1 to 4) over a period of 4 days p.i. (A) Serial dilutions of the DNA preparations were blotted onto a nylon membrane and hybridized to a radiolabelled probe corresponding to the Ad5 pIX and IVa2 regions. Each line corresponds to a time p.i. (day 0 to 4 from top to bottom), whereas serial dilutions of the DNA preparations are arranged in vertical rows (1:1 to 1:100 from left to right). (B) Southern analysis of *Nde*I-restricted low-molecular-weight DNA from Hep3B cells infected with AdE3+βGal or AdβGal/dl1007 at an MOI of 20 TDU/cell. Viral DNA from ca. 2×10^5 cells was digested with *Nde*I and subjected to Southern analysis with a radiolabelled AdRSVβGal genomic probe. The sizes (in base pairs) and positions of the $E4^+$ *Nde*I fragment of AdE3+βGal (4,847 bp) and the $E4^-$ *Nde*I fragment of AdβGal/dl1007 (2,968 bp) are indicated.

Replication of virus DNA in nonpermissive cells of human origin. We first compared the abilities of different tumor-derived cell lines of human origin (Hep3B, HeLa, KB, and HepG2) to sustain viral DNA accumulation following infection with an E1-deleted virus. A quantitative slot blot assay was used for this comparison; low-molecular-weight DNA was extracted (26) at different times p.i. and hybridized with an Ad5-specific radiolabelled probe (see Materials and Methods). A typical slot blot analysis carried out on Hep3B cells is shown in Fig. 2A. Upon AdE3+βGal infection at an MOI of 20 TDU/cell, a significant increase in the amount of viral DNA was detected as early as 48 h p.i. and peaked at 72 h to more than 30-fold the initial amount. AdE3+βGal DNA levels did not increase beyond 72 h p.i., very likely because extensive cell damage occurred as early as 3 days p.i. and led to cell detachment (see below). The quantity of viral DNA initially applied to the cells was less than twofold higher than that detected at 6 h p.i., indicating that the 30-fold increase of AdE3+βGal DNA that occurred following infection did reflect some kind of replication. This conclusion was further supported by the absence of viral DNA accumulation when araC, a known inhibitor of adenovirus DNA replication, was included in the culture medium (see Fig. 7A). In contrast with the case for AdE3+βGal, infection with any of the E1/E4-defective viruses under identical conditions (20 TDU/cell) showed no or very little increase of intracellular viral DNA over a period of 4 days p.i. Note that the cells had been similarly infected with the E1- or E1/E4-defective viruses as demonstrated by similar amounts of viral DNA at 6 h p.i. (Fig. 2A), together with a similar number of *lacZ*-expressing cells following infection (see Fig. 6). DNA extracts were also subjected to *Nde*I restriction and Southern analyses with an AdRSVβGal-specific radiolabelled probe. Typical results are shown in Fig. 2B for AdE3+βGal and AdβGal/dl1007 over a period of 4 days p.i. Notably, restriction patterns confirmed the identity of the infecting viruses and that the cells had been similarly infected. Again, an important increase was apparent 2 days p.i. with AdE3+βGal DNA but not with the E1/E4-defective virus. The results also indicate a stoichiometric proportion of the restriction fragments, indicating that replication of AdE3+βGal DNA resulted not from abortive cycles but rather from a bona fide replication of full-length genomes. Densitometric quantifications of the restriction fragments indicated levels of AdβGal/dl1007 DNA that were roughly 20- to 30-fold lower than those of AdE3+βGal at 4 days p.i., in good agreement with the quantification of the slot blots.

Comparison of early and late viral gene expression. Adenovirus DNA replication is dependent upon the E2A-encoded 72-kDa DNA binding protein (50). We have used Northern blot analysis to compare the levels of E2A mRNA in cells infected with AdE3+βGal or the doubly defective viruses. As a loading and transfer control for all Northern blotting experiments in this study, membranes were systematically hybridized to a radiolabelled probe specific to the β-actin mRNA, as its steady-state level is not greatly affected by infection with an E4-competent or an E4-defective adenovirus (42). As shown in Fig. 3, Hep3B cells exhibited higher levels of E2A-specific RNAs at 48 h p.i. with the E4-competent virus (compare lane 2 with lanes 3 to 6), in agreement with the larger amount of AdE3+βGal DNA detected at this time (Fig. 2). Again, there was no significant difference between the doubly E1/E4-defective viruses that were tested, including AdβGal/dl1014, which exhibits a deletion within E4 that is associated, in the presence of an

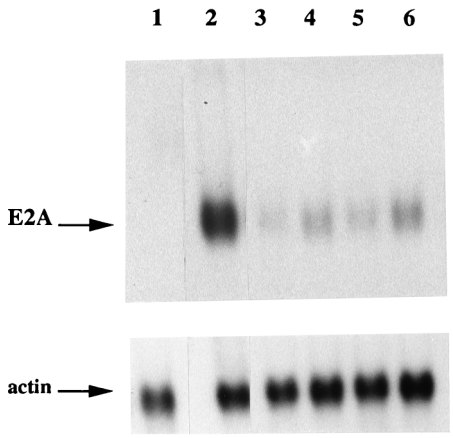

FIG. 3. Comparative analysis of E2A-specific RNAs in Hep3B cells. Cells were infected at an MOI of 20 TDU/cell with the E1- or E1/E4-defective viruses. Total cellular RNA was prepared 48 h p.i., and poly(A)$^+$ RNA was isolated by oligo(dT) selection. Each lane contained 2.5 μg of poly(A)$^+$ RNA fractionated by electrophoresis through a 1% agarose–0.66 M formaldehyde gel and transferred to a nylon membrane. The membrane was hybridized first to a ^{32}P-labelled actin antisense RNA probe (lower panel) and then, following removal of the actin probe, to a ^{32}P-labelled E2A antisense RNA probe (upper panel). The expected position of the E2A mRNAs is indicated. Lane 1, mock-infected cells; lane 2, AdE3+βGal; lane 3, AdβGal/dl1004; lane 4, AdβGal/dl1007; lane 5, AdβGal/dl1011; lane 6, AdβGal/dl1014.

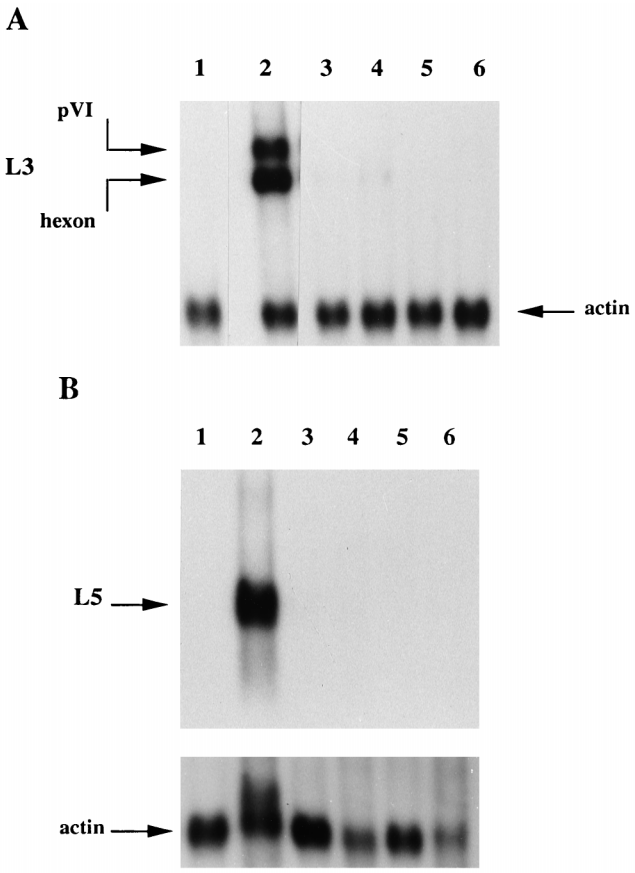

FIG. 4. Comparative analysis of late gene expression in Hep3B cells. Total cellular RNA was prepared 48 h after infection of Hep3B cells with the E1- or E1/E4-defective viruses at an MOI of 20 TDU/cell. Polyadenylated RNA was isolated and analyzed as described for Fig. 3 with a ^{32}P-labelled antisense RNA probe for L3 (A) or L5 (B) transcripts. Cells were infected with the following viruses: lane 2, AdE3+βGal; lane 3, AdβGal/dl1004; lane 4, AdβGal/dl1007; lane 5, AdβGal/dl1011; lane 6, AdβGal/dl1014; lane 1, none (mock-infected cells). Each lane contained 2.5 μg of poly(A)$^+$ RNA. The expected positions of the pIV and hexon L3 mRNAs and of the fiber L5 mRNA are indicated. Following hybridization with the L3 or L5 probe, membranes were hybridized (without removal of the previous probe) with a ^{32}P-labelled antisense RNA probe for actin mRNAs. Actin signals are shown below panel B, as signals for fiber and actin mRNAs overlap due to their similar sizes.

intact E1 region, with a severe impairment of DNA replication in HeLa cells (6).

We next assessed the consequences for late gene expression that were associated with the deletion of E4 sequences from the backbone. L3 (pVI and hexon)- and L5 (fiber)-specific RNAs were analyzed by Northern blotting of poly(A)$^+$ RNAs from Hep3B cells infected at an MOI of 20 TDU/cell. Infection with the AdE3+βGal virus was associated with significant levels of pVI (4.6-kb) and hexon (3.8-kb) L3 mRNAs at 48 h p.i. (Fig. 4A, lane 2). In contrast, these species were not detected when the cells were infected with any of the E1/E4-defective viruses (Fig. 4A, lanes 3 to 6). Exposure of the film for 60 h instead of 6 h was required to detect faint signals that corresponded to these late mRNAs (data not shown). When the same RNA preparations were hybridized to a probe specific for the 2.5-kb fiber-encoding mRNA (L5), similar differences were evident depending on the presence or absence of a functional E4 region within the viral backbone: fiber-specific poly(A)$^+$ RNAs were unambiguously detected in AdE3+βGal-infected cell extracts (Fig. 4B, lane 2) but not when the E1/E4-defective viruses were used (lanes 3 to 6), even after longer exposures of the film. Immunoprecipitation experiments also demonstrated hexon protein synthesis as early as 2 days p.i. with the E1-deleted virus, but not the doubly defective virus, even after 6 days (Fig. 5).

Phenotypic consequences of viral infection. A remarkable feature that emerged during the course of this study is that infection of nonpermissive cells with an E1- or an E1/E4-defective virus was associated under our experimental conditions with different outcomes with regard to cell morphology and survival. For example, infection of Hep3B cells with AdE3+βGal at an MOI of 20 TDU/cell resulted in phenotypic abnormalities as early as 3 days p.i.: a large number of cells had detached from their support, while most of the remaining cells exhibited evidence of cell enlargement, rounding, and clumping (Fig 6D). These cellular abnormalities were also observed following infection with another E1-deleted adenovirus (AdRSV/βGal) and no matter what process was used to prepare the stocks (see Materials and Methods). In contrast, there was no apparent virus-induced cytotoxicity following infection with AdβGal/dl1007 (20 TDU/cell, corresponding to the same number of *lacZ*-expressing cells at 48 h p.i.) (compare Fig. 6A and B). Four days after infection, i.e., at a time when AdE3+βGal-infected cells were almost completely detached (Fig. 6G), AdβGal/dl1007-infected cells appeared to be as healthy as their mock-infected counterparts. This was also true 5 days after infection (compare Fig. 6F and H), after which both mock- and AdβGal/dl1007-infected cell monolayers started to exhibit signs of cell deterioration. Again, AdβGal/dl1004, AdβGal/dl1011, and AdβGal/dl1014 behaved similarly to AdβGal/dl1007 in this assay.

Quantitative analysis of *lacZ* expression in vitro. A quantitative β-galactosidase assay was used to compare the abilities of AdE3+βGal and E1/E4-defective viruses to express their transgene following infection. Experiments were carried out in the presence of araC to prevent any bias resulting from different levels of viral DNA accumulation following infection with either type of virus. Under the conditions used (20 TDU/cell in

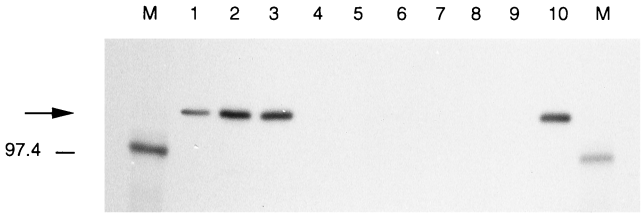

FIG. 5. Comparative analysis of de novo hexon synthesis in Hep3B cells. Hep3B cells infected with AdE3+βGal (lanes 1 and 2) or AdβGal/dl1007 (lanes 5 to 9) at an MOI of 20 TDU/cell were labelled at the indicated times p.i. with [^{35}S]methionine for 24 h and extracted with radioimmunoprecipitation assay buffer. Equal amounts, as assessed by trichloroacetic acid-precipitable radioactivity, were subjected to immunoprecipitation with an antihexon antibody and analyzed on an SDS–6% polyacrylamide gel, except for lanes 3 and 10, for which 2.5 times less material was loaded. Labelling was initiated at the following times p.i.: lanes 1 and 5, 2 days; lanes 2 and 6, 3 days; lane 7, 4 days; lane 8, 5 days; and lane 9, 6 days. Lane 4, extracts from Hep3B mock-infected cells; lanes 3 and 10, 293 cells infected with AdRSVβGal (10 TDU/cell) and labelled for 24 h at 24 h p.i.; lanes M, molecular weight markers (in thousands).

the presence of 50 μg of araC per ml), there was no increase of viral DNA in infected Hep3B cells during the entire time course of the experiment (Fig. 7A), and this translated into kinetics and levels of β-galactosidase specific activity that were not significantly different following infection with AdE3+βGal or AdβGal/dl1007 (Fig. 7B).

Assessment of the *lacZ*-transgenic mouse model. The relative importance of the transgene versus viral proteins in the immune clearance of the virally infected cells in mice is a complex issue that has led to different conclusions with different strains of mice (49, 58). We have addressed this issue with C57BL/6 mice, a genetic background particularly responsive to adenovirus infections (19). As a prerequisite, we assessed the relevance of a *lacZ*-transgenic line (9) with a C57BL/6 genetic background to compare our *lacZ* recombinant adenoviruses. We first verified that there was no detectable expression of the *lacZ* transgene in the livers of noninfected adults and that systemic administration of a non-*lacZ* E1-defective recombinant adenovirus did not upregulate expression of the endoge-

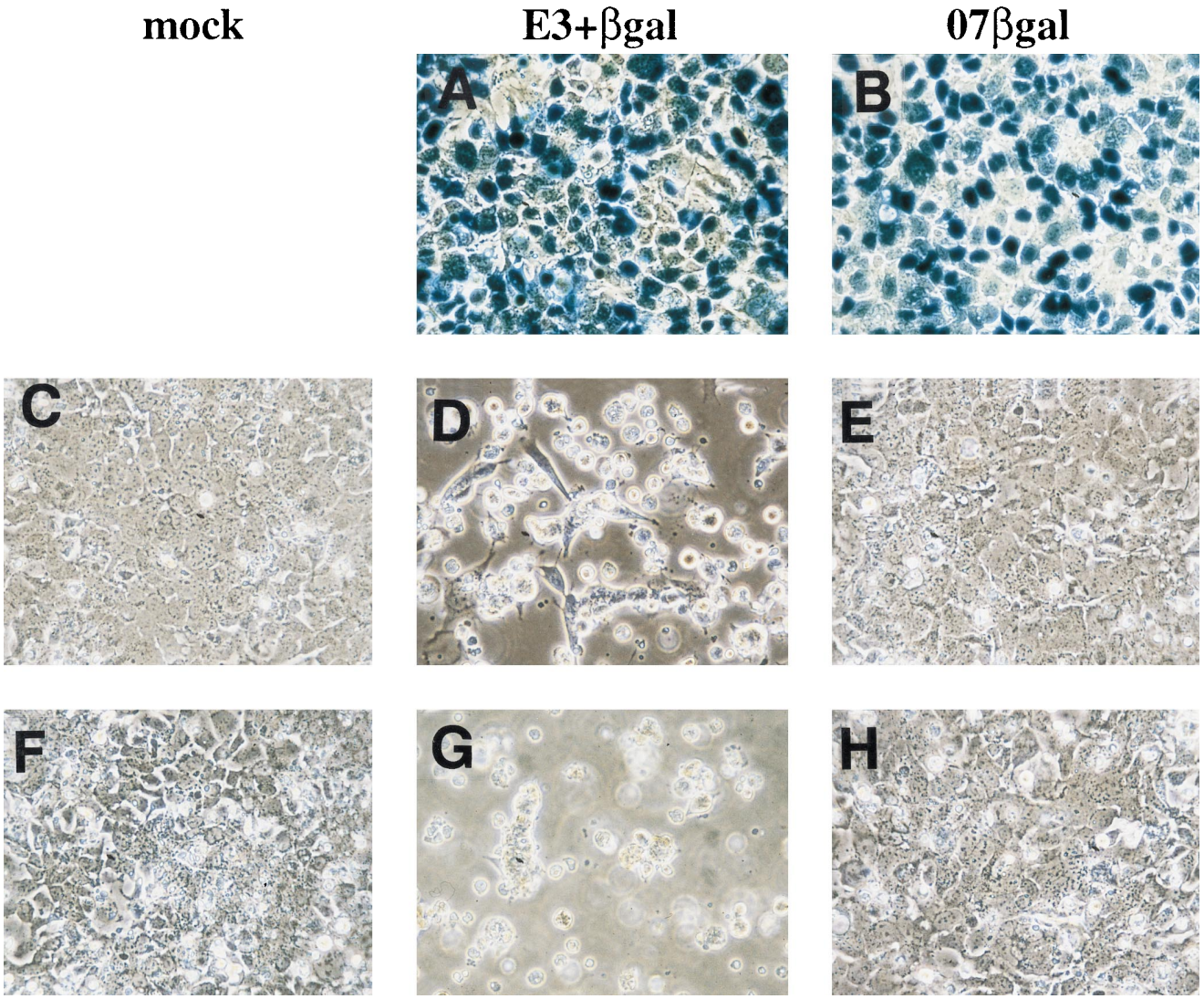

FIG. 6. Virus-induced cytotoxicity in Hep3B cells. Subconfluent monolayers of Hep3B cells grown in 100-mm-diameter dishes were mock infected (C and F) or infected with AdE3+βGal (A, D, and G) or AdβGal/dl1007 (B, E, and H) at an MOI of 20 TDU/cell. Control dishes were stained with X-Gal at 48 h p.i. and photographed under phase-contrast microscopy at 60 h p.i. (A and B). Test dishes were photographed under phase-contrast microscopy at day 3 (C, D, and E), 4 (G), or 5 (F and H) p.i. Magnification, ×250.

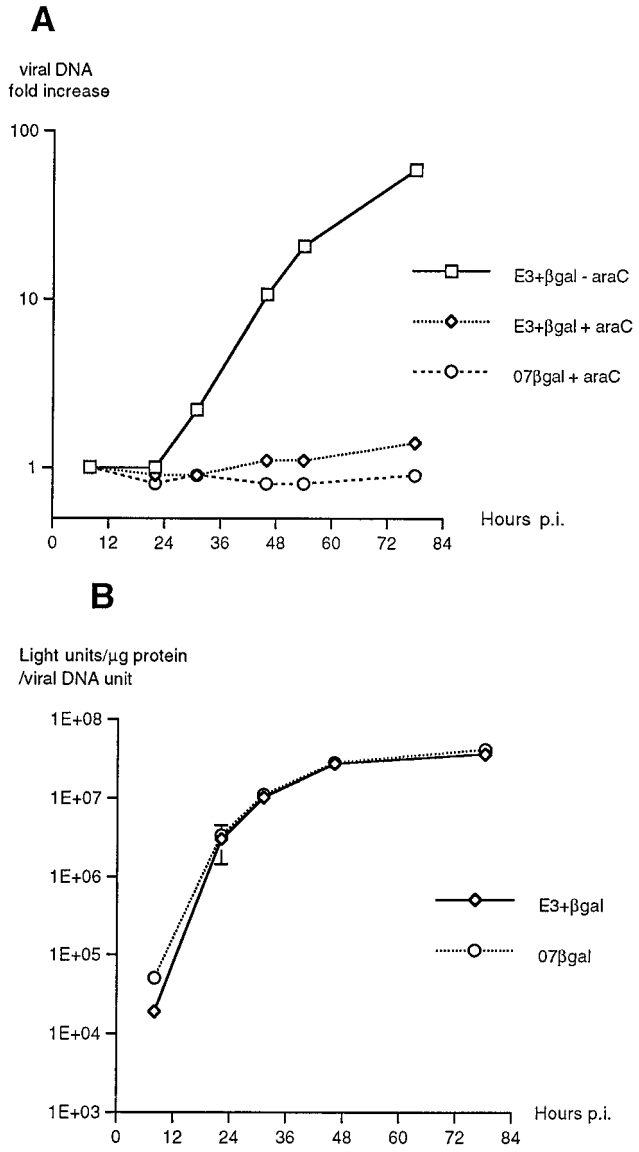

FIG. 7. Comparative analysis of β-galactosidase expression in Hep3B cells. Hep3B cells were infected with AdE3+βGal or AdβGal/dl1007 at an MOI of 20 TDU/cell in the absence or presence of araC (see Materials and Methods). Cell extracts were prepared at 8, 22, 31, 46, and 78 h p.i. for β-galactosidase activity quantification in a chemiluminescence assay, and viral DNA accumulation was monitored in parallel on control dishes. (A) Quantification of viral DNA accumulation in the absence or presence of araC. Results are expressed as the ratio between the amount of viral DNA at different times p.i. and the amount at 8 h p.i. (B) Quantification of β-galactosidase activity as measured in the presence of araC. Results (light units per microgram of protein per arbitrary unit of viral DNA) are presented as means of triplicate determinations with standard deviations.

nous *lacZ* gene (data not shown). Next, 2.5×10^9 TDU of AdE3+βGal was infused via the tail veins of C57BL/6 mice and C57BL/6 *lacZ*-transgenic mice (TG mice), and the number of X-Gal-positive hepatocytes was monitored by histochemical staining (Table 1). Infusion of the virus led to drastic differences in the persistence of βgalactosidase-positive hepatocytes in the two strains of mice. In the nontransgenic mice, the numbers dropped from 80 to 8% over a 24-day period and there were almost no remaining X-Gal-positive hepatocytes at day 45 p.i. In contrast, 50 and 33% of hepatocytes from the TG mice still scored positive at 24 and 45 days p.i., respectively.

TABLE 1. Morphometric analysis of liver sections from C57BL/6 background mice for *lacZ* expression following administration of AdE3+βGal

Mouse strain	% *lacZ*-positive hepatocytes[a] (*n*) on day p.i.:				
	4	14	24	45	88
C57BL/6	80 ± 5 (2)	55 ± 10.5 (3)	8 ± 1.5 (3)	<1 (3)	ND
TG	80 ± 0.5 (3)	ND[b]	50 ± 16 (3)	33 ± 4.5 (3)	16 ± 2 (3)
C57BL/6 nude	90 ± 0.5 (2)	ND	45 ± 5 (2)	ND	ND

[a] Data were quantified by analyzing for each animal 10 liver sections representing a total of ca. 1,000 hepatocytes; results are shown as means ± standard deviations.
[b] ND, not determined.

To assess the extent of virus-induced inflammation and necrosis that developed within the liver, we have developed a reproducible scoring system (see Materials and Methods). The virus-induced inflammatory response of normal C57BL/6 mice was scored as minimal (grade 1) 4 days p.i., whereas multiple large intraparenchymatous lymphocyte foci that were associated with plasmocytes were apparent at day 24 p.i. (see Fig. 9A). Inflammation was scored severe (grade 4) (Fig. 8C) at this time and then gradually decreased to grade 2 between days 24 and 66 p.i. The overall response of the TG mice to AdE3+βGal infection was significantly reduced: while the reaction of the non-TG mice was severe (grade 4) at day 24 p.i., that of the TG mice was scored as only mild (grade 2) (compare Fig. 8C and D; see also Fig. 9A). At day 45, inflammation was also significantly reduced in the transgenic animals (Fig. 9A), and it was minimal at day 66 p.i. (Fig. 9A). The fact that inflammation triggered by an E1-deleted *lacZ*-encoding virus was reduced from severe (grade 4) to mild (grade 2) in the TG animals implicates the immune status of the host with regard to the *Escherichia coli* protein as a major determinant of the disappearance of the transduced hepatocytes in the C57BL/6 genetic background. The fact that the decreases of the X-Gal-positive hepatocytes between 4 and 24 days p.i. were very similar when AdE3+βGal was injected into C57BL/6 nude mice or the TG mice (Table 1) further supports this conclusion.

The additional inactivation of E4 allows long-term gene delivery in mouse liver. The TG mice were therefore used as a model to assess the behavior of *lacZ*-expressing E1- or E1/E4-defective recombinants in the liver. TG mice were infused with AdβGal/dl1007 (4.6×10^9 TDU) or AdE3+βGal (2.5×10^9 TDU) via the tail vein, as these doses were previously shown by X-Gal staining to transduce identical proportions of hepatocytes (75 to 80%) at 4 days p.i. Total cellular DNA from infected liver extracts was prepared and analyzed by slot blot and Southern analyses. Quantification of the viral DNA within the liver extracts indicated similar amounts 4 days after infection with either virus. Persistence of AdE3+βGal DNA in the livers of the TG mice declined in a manner similar to that of the B-galactosidase-positive hepatocytes: 51, 26, and 14% of the amount of DNA at day 4 p.i. were detected 24, 45, and 88 days p.i., respectively (Fig. 10A). In contrast, AdβGal/dl1007 DNA was very stable, as 76% of the amount at day 4 p.i. was still present at day 88 p.i. Southern blotting of *Not*I- or *Sal*I-restricted low-molecular-weight DNA from the infected liver confirmed the identity of the infecting virus. Furthermore, viral DNA was extrachromosomal, and it was not circularized or fragmented (Fig. 10B). Because the enzymes used are inhibited by methylation of CpG dinucleotides, we also concluded that none of the *Not*I and *Sal*I sites in the vector backbone were methylated, including those present in the RSV LTR.

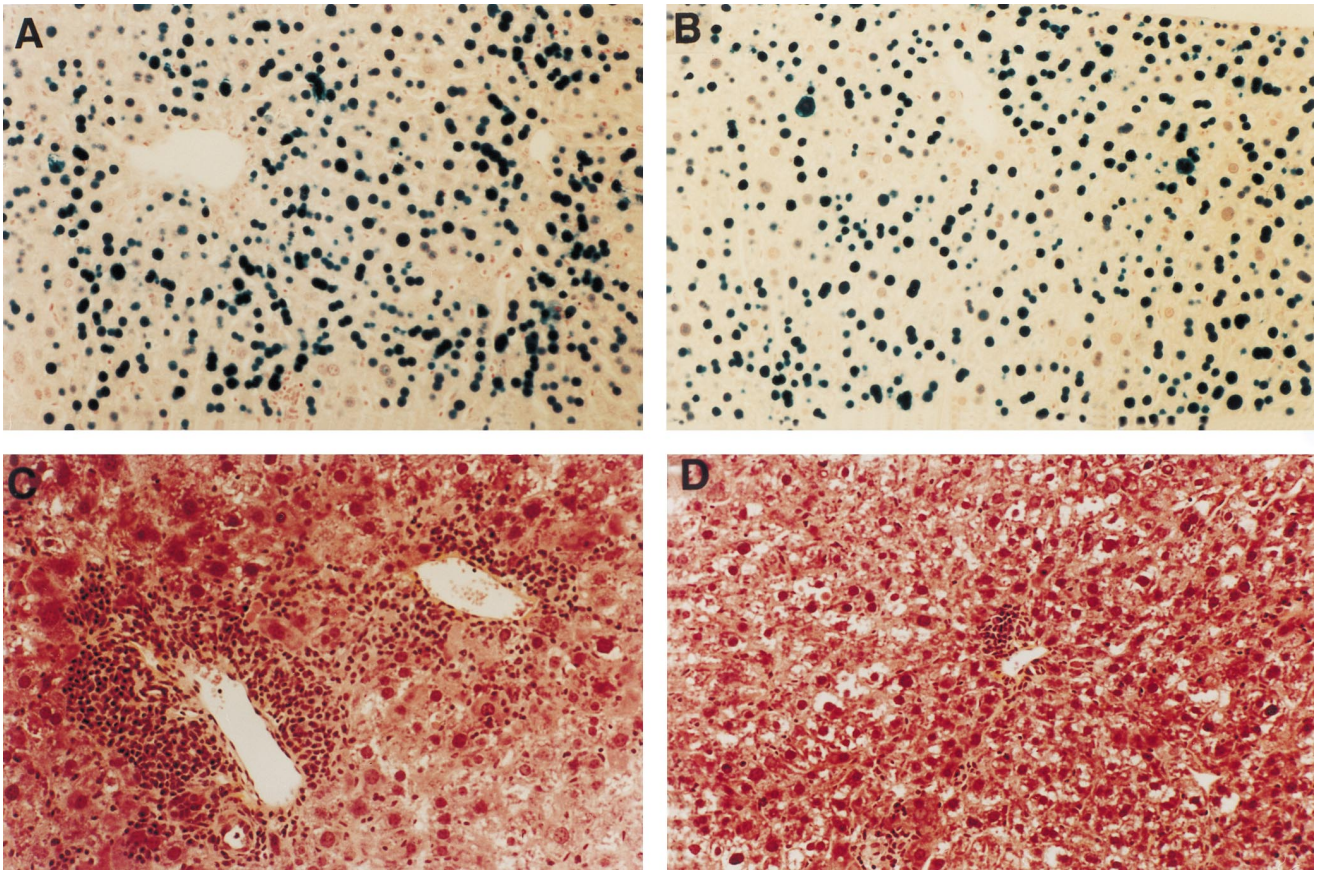

FIG. 8. Histological analysis of liver sections of mice injected with AdE3+βGal. AdE3+βGal (2.5×10^9 TDU) was injected via the tail vein, and mice were sacrificed at day 4 (A and B) or 25 (C and D) p.i. Livers were fixed in 4% paraformaldehyde and stained for evaluation of β-galactosidase activity. By day 4, C57BL/6 (A) and TG (B) mouse livers exhibited the same proportion of β-galactosidase-positive cells (75 to 80%), while infection with a non-*lacZ*-encoding adenovirus led to X-Gal-negative hepatocytes (not shown). Liver histology (hematoxylin and eosin staining) was also assessed for each sample. A typical representation of the virus-induced inflammation is shown at day 25 p.i. A massive intraparenchymatous lymphocyte infiltration, which nearly subsided by day 66 p.i., is observed in C57BL/6 mice (C). Small foci scattered throughout the liver are observed following infection of TG mice (D).

Despite the remarkable persistence of AdβGal/dl1007 DNA in the liver, the number of X-Gal-positive hepatocytes dramatically decreased to 3.5% by day 24 and remained below 1% thereafter (Table 2). For AdE3+βGal and AdβGal/dl1007, the kinetics of β-galactosidase specific activity (units per milligram of liver extract) was identical to that of the X-Gal-positive hepatocytes (data not shown). The rapid loss of transgene expression that followed injection of AdβGal/dl1007 into TG mice was not restricted to the extent of the E4 deletion harbored by this particular doubly E1/E4-defective virus. Indeed, transgene expression had almost reached background levels 24 days after administration of AdβGal/dl1004 or AdβGal/dl1014 (Table 2), although the viral DNA was still present (data not shown). Compared to the case for the E1-deleted control virus, infusion of the doubly defective adenoviruses into the TG mice promoted little (if any) inflammation (Fig. 9B) and necrosis (Fig. 9C). For AdβGal/dl1004, inflammation at day 24 p.i. was scored as mild for two of three animals (Fig. 9B). Interestingly, the mild inflammation that was observed in these two animals was also correlated with a higher fraction of X-Gal-positive hepatocytes (7%).

DISCUSSION

We have assessed the consequences of inactivating E4 from virus AdE3+βGal, an E1-deleted virus expressing a nucleus-targeted B-galactosidase from the RSV LTR. The structural and functional complexities of the E4 regulatory locus prompted us to study a set of isogenic viruses (AdβGal/dl1004, AdβGal/dl1007, AdβGal/dl1011, and AdβGal/dl1014) lacking both E4orf3 and E4orf6 but otherwise retaining various coding potentials from the E1A-inducible E4 promoter (Fig. 1). The recombinant adenoviruses were first compared in vitro under identical infection conditions. Compared to the E1-deleted control virus, infection with the doubly defective adenoviruses was associated in Hep3B cells with an impaired ability to replicate and express the viral genome, together with the extinction of virus-induced cytopathic effects. On the other hand, specific expression of the transgene was quantitatively unchanged in a short-term assay. As far as we can tell, all four E1/E4-defective viruses behaved identically, including AdβGal/dl1014 ($E4orf4^+$), which exhibits a deletion that has been shown to inhibit viral DNA replication in HeLa cells (6). This unexpected observation may result from the use of a different indicator cell line or because our construct also has a deletion within E1.

Our in vitro data truly reflect the additional consequences of inactivating the E4 function per se, because identical amounts of infectious viruses were used and led to (i) comparable transductions (Fig. 6) and (ii) similar intracellular amounts of viral DNA at 6 hours p.i. (Fig. 2). The lower replication of viral

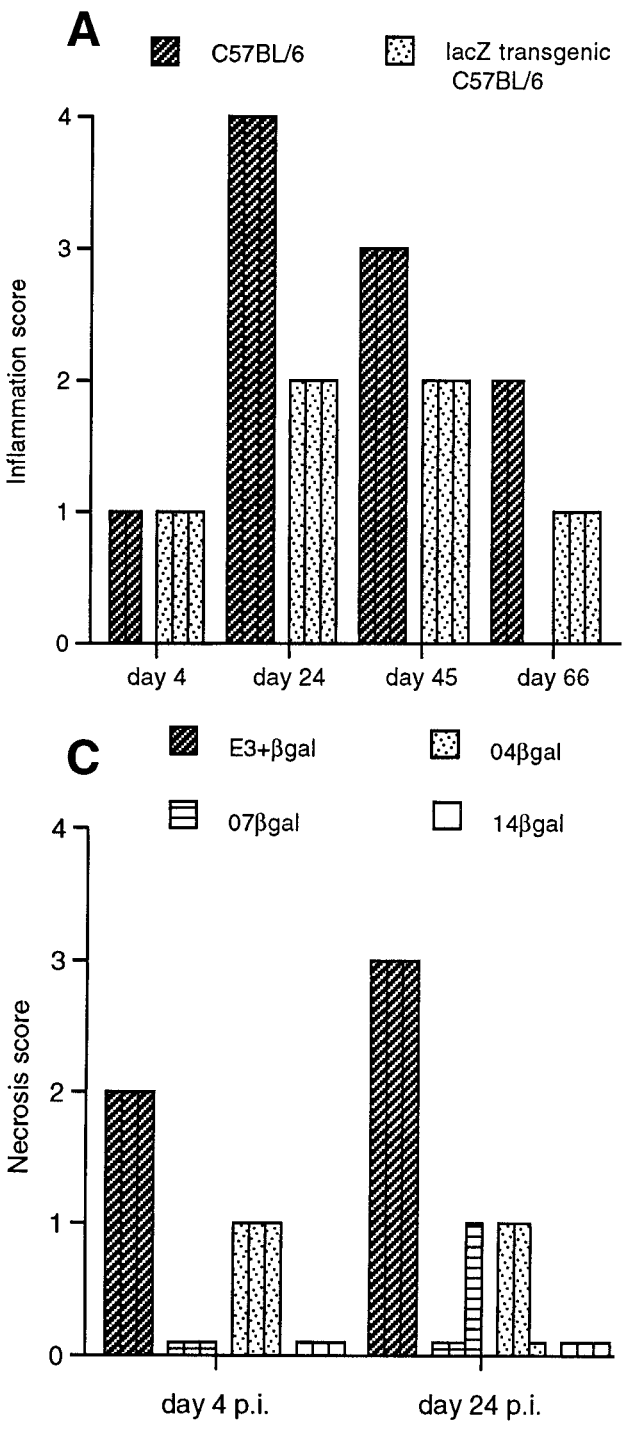

FIG. 9. Quantification of virus-induced inflammation and necrosis in livers of mice injected with E1- or E1/E4-defective viruses. A reproducible scoring system was developed to assess virus-induced inflammation and necrosis in the livers of mice infused with E1- or E1/E4-defective viruses (see Materials and Methods). Bars represent individual scores ($n = 2$ or 3); the scores for animals showing no signs of virus-induced inflammation or necrosis (grade 0) were artificially elevated to a value of 0.1 to differentiate them from nonavailable data. (A) Inflammation score in C57BL/6 and TG mice infused with AdE3+βGal (2.5×10^9 TDU). (B and C) Inflammation and necrosis scores, respectively, in TG mice infused with the indicated E1- or E1/E4-defective viruses. See Table 2 for the injected doses and the percentages of *lacZ*-positive hepatocytes at the indicated times p.i. Typical grade 4 and grade 2 inflammations are illustrated in Fig. 8C and D, respectively.

DNA in cells infected with a doubly defective virus was in accordance with lower levels of E2A RNAs (Fig. 3) and protein (72-kDa DNA binding protein) as assessed by specific immunoprecipitation experiments (11). Because E2A expression is dependent upon two pathways controlled by early regions 1A (E1A) and 4 (E4orf6/7) and because to our knowledge there is no evidence of a cellular activity that could substitute for E4orf6/7, expression of E2A following Hep3B infection with a virus lacking both functions is most likely the consequence of endogenous E1A-substituting factors of viral (44) and/or cellular (46) origin. Similar E1A-substituting activities may be widely present in human cells, as AdE3+βGal DNA accumulated in all tested tumor-derived cell lines, including HepG2 (liver), HeLa (cervix), and KB (upper digestive tract) cells: a 25 (HeLa and KB)- to 60 (HepG2)-fold increase was observed between 3 and 4 days p.i. at an MOI that transduced between 70 and 90% of the cells. At a time when AdE3+βGal DNA had reached its peak level, infection with the doubly defective adenoviruses led to a 3 (HeLa and KB)- to 15 (Hep3B and HepG2)-fold reduction of the viral genomes.

Dual inactivation of E4orf3 and E4orf6 directly or indirectly hampers the cytoplasmic accumulation of late adenovirus mRNAs (5, 23, 25). We did not find evidence that an endogenous activity could efficiently substitute for this adenovirus regulatory activity. Indeed, infection of Hep3B cells with a doubly defective virus resulted in an almost complete shutdown in the steady-state levels of L3 (pVI- and hexon-encoding) and L5 (fiber-encoding) poly(A)$^+$ RNAs at 48 h p.i. as compared to those observed when AdE3+βGal was used (Fig. 4). Reduction of late gene expression also occurred at the protein level as shown for the L3-encoded hexon protein (Fig. 5). AdE3+βGal infection was also associated with the development of morphological alterations that ultimately led to cell death (Fig. 6). In contrast, no cytotoxicity was observed when identical doses of doubly defective viruses were used. In vivo detrimen-

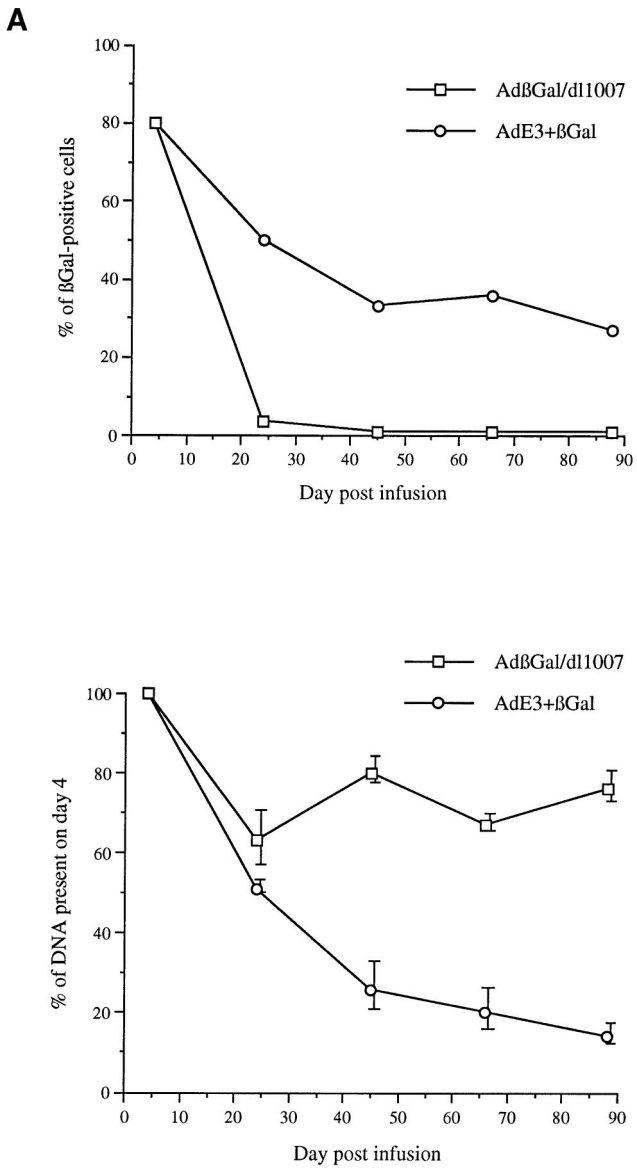

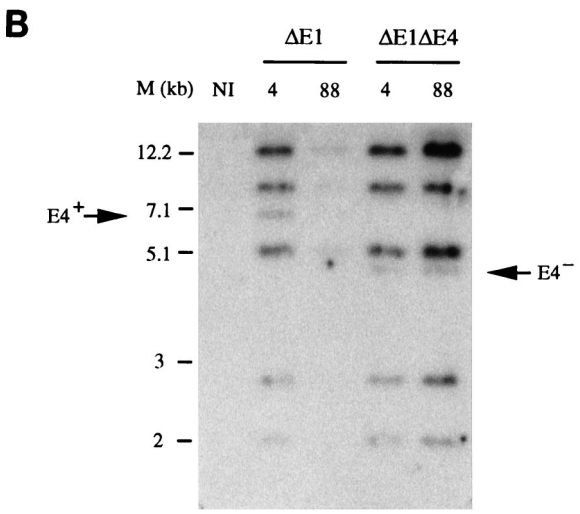

FIG. 10. Persistence of viral DNA in the livers of TG mice injected with AdE3+βGal or AdβGal/dl1007. AdE3+βGal (2.5×10^9 TDU) or AdβGal/dl1007 (4.6×10^9 TDU) virus was administered to TG mice via tail vein injection. (A) At the indicated times p.i., the animals were sacrificed to quantify the viral DNA in the liver by a slot blot assay. Three animals were injected for each time point, except for AdβGal/dl1007-infected mice at days 24, 45, and 88 p.i. ($n = 2$). The mean value and its standard deviation are shown. The quantity of AdβGal/dl1007 DNA at day 4 p.i. was slightly higher than that of AdE3+βGal DNA (ratio = 1.13); it was normalized to 100% for both viruses for simplicity. βGal, β-galactosidase. (B) Southern analysis of AdE3+βGal and AdβGal/dl1007 DNAs. Total cellular DNA from the liver of a representative injected animal was prepared at 4 or 88 days p.i., digested with *Not*I, and subjected to Southern analysis (20 μg per lane). The radiolabelled probe corresponds to *Not*I restriction fragments from the AdRSVβGal virus, which lacks an internal *Xba*I fragment within the E3 region (48). ΔE1 and ΔE1ΔE4, TG mice infected with AdE3+βGal and AdβGal/dl1007, respectively. The lane numbering indicates the day of sacrifice p.i. NI, liver of a noninfected transgenic animal. The positions of the 6.4-kb $E4^+$ (AdE3+βGal) and 4.5-kb $E4^-$ (AdβGal/dl1007) *Not*I restriction fragments are indicated by arrows. These fragments encompass the E3 deletion of the radiolabelled probe, and their signals are less intense than those of the other *Not*I fragments. The migrations and molecular size of particular fragments from the 1-kb ladder (Gibco BRL) are indicated on the left.

tal effects on cell viability that could result from the sole deletion of E1 from the adenovirus backbone may represent adjuvant side effects for cytotoxic antitumoral gene therapy approaches. On the other hand, the E4orf6 protein has been reported to inhibit the transactivation activity of p53 in vitro (13), a function required for its tumor-suppressing activity (61). A direct (cytotoxic) or indirect (e.g., cytotoxic-T-lymphocyte-mediated) clearance of the infected cells that would result from the accumulation of viral proteins is also certainly not optimal for treatment of genetic deficiency disorders (e.g., cystic fibrosis), for which a conservative approach is needed. At least in this respect, the additional inactivation of E4 from the vector backbone may prove beneficial.

The murine response to recombinant adenoviruses is a complex event that hampers long-term survival of the transduced cells. Barr et al. (3) have reported a remarkable variability in the persistance of transgene expression, ranging from several weeks to more than 3 months when an E1-deleted adenovirus expressing human α-antitrypsin was infused into different inbred strains of mice. In another study, human erythropoietin expressed from an E1-deleted recombinant adenovirus injected intramuscularly was recognized as immunogenic, thereby limiting the efficacy of gene delivery in CD1-mice (49). Another study using *lacZ*-transgenic mice (ROSA-26) injected with an E1-deleted *lacZ* recombinant adenovirus led to the conclusion that cytotoxic T lymphocytes specific to viral antigens were mostly responsible for the clearance of the transduced cells in vivo, while those directed against the *E. coli* β-galactosidase played a minor role (58). The behaviors of the recombinant adenoviruses in this study have been compared in the livers of C57BL/6 mice, a genetic background which responds to adenovirus infection by mounting a strong, biphasic, cellular infiltration (19). As a prerequisite, we have identified a C57BL/6 *lacZ*-transgenic line in which AdE3+βGal-infected hepatocytes persisted in a manner similar to that in *nu/nu* mice backcrossed in the same genetic background (Table 1). Based on the results of our in vitro study, we anticipated that E1- and E1/E4-defective adenoviruses would exhibit different behaviors in the livers of these model animals. This proved to be the case, as the additional deletion of E4 promoted the persistence of the viral chromosome for at least 3 months in the liver (Fig. 10A). Molecular characterization demonstrated that viral DNA was extrachromosomal, linear, and nonmethylated (Fig. 10B).

TABLE 2. Morphometric analysis of C57BL/6 and TG liver sections for *lacZ* expression following administration of E1- or E1/E4-defective adenovirus vectors

Day post-injection	Virus[b]	% *lacZ*-positive hepatocytes[a] (*n*) in:	
		TG mice	C57BL/6 mice
4			
	AdE3+βGal	80 ± 0.5 (3)	80 ± 5 (2)
	AdβGal/dl1007	80 ± 8 (3)	63 ± 12.5 (3)
	AdβGal/dl1004	90 ± 7 (3)	ND[c]
	AdβGal/dl1014	40 ± 0.5 (3)	ND
24			
	AdE3+βGal	50 ± 16 (3)	8 ± 1.5 (3)
	AdβGal/dl1007	3.5 ± 0.5 (2)	<1 (3)
	AdβGal/dl1004	5.6 ± 2 (3)	ND
	AdβGal/dl1014	1 ± 0.5 (3)	ND

[a] Data were determined as described in Table 1, footnote *a*.
[b] Doses were 2.5×10^9 TDU for AdE3+βGal, 4.6×10^9 TDU for AdβGal/dl1007 and AdβGal/dl1004, and 4×10^9 TDU for AdβGal/dl1014.
[c] ND, not determined.

Long-term persistence of the viral DNA in the liver was not associated with a sustained expression of β-galactosidase. A similar decline in transgene expression was also noted independently of the extent of the deletion within E4 (Table 2). Although we cannot formally exclude the possibility that inactivation of E4 resulted in the removal from the viral backbone of *cis* or *trans* elements required for long-term gene expression, we favor the hypothesis that rapid extinction of transgene expression from the doubly defective viruses resulted from the use of the RSV LTR to drive its expression. Independent observations actually support the low activity of this promoter in primary hepatocytes in vitro and in vivo (29, 33, 39). In particular, Overbeek et al. (38) reported that an RSV enhancer/promoter-chloramphenicol acetyltransferase gene construct was functional in many organs but not in the livers of five independent strains of transgenic mice. The RSV LTR contains multiple transcription factor binding sites, including CCAAT/enhancer elements, CArG motifs, and C/EBP binding sites, and it has been previously demonstrated that RSV LTR-driven expression could be induced in vitro by addition of serum and during cellular proliferation (31, 41). The fact that the E1/E4-defective recombinants in this study did not promote a sustained inflammation or necrosis within the livers of the transgenic mice (Fig. 9B and C) fits with a progressive downregulation of RSV LTR-driven *lacZ* expression following infection (Table 2). Our observations also imply that administration of either type of virus did initially upregulate the RSV LTR, presumably because of the inflammatory nature of the virus input, leading to similar numbers of X-Gal-positive hepatocytes at 4 days p.i. (Table 2). Such an inflammation-induced expression has been previously observed in the livers of mice injected with an E1-deleted recombinant adenovirus whose transgene expression was driven by acute-phase-responsive promoters (51). During the course of the present study, a paper has appeared in which it was reported that a doubly defective virus, identical to AdβGal/dl1004 except that transgene expression was driven by a composite cytomegalovirus enhancer/β-actin promoter, was capable of promoting β-galactosidase expression for at least 2 months in hepatocytes from ROSA-26 mice with a mixed C57BL/6-129 genetic background (18). That study and the present study suggest that the additional inactivation of E4 is a prerequisite for stable gene delivery in mouse liver and that the viral backbone is not sequestered in a subcellular compartment that would hamper long-term transgene expression.

ACKNOWLEDGMENTS

We thank S. Benoist, N. Couteault, N. Di Falco, S. Falzon, A. Gaumet, and N. Ratet for technical assistance, N. Hanania and I. Redchenko for providing the L3 transcription plasmid, M. Lakich for helpful discussion and critical reading of the manuscript, and G. Ketner (Baltimore, Md.) for providing us with H5dl1004, H5dl1007, H5dl1011, and H5dl1014. We thank C. Babinet (Institut Pasteur, Paris, France) for providing us with the TG mice and P. Hardouin (IGR, Villejuif, France) and P. Gallix (CRVA, Vitry-sur-Seine, France) for animal care. We thank J. Crouzet, P. Denèfle, J. B. Le Pecq, and J. F. Mayaux for their constant interest and support.

This work was part of the BioAvenir program supported by Rhône-Poulenc, the French Ministry of Research, and the French Ministry of Industry.

REFERENCES

1. **Babiss, L. E., H. S. Ginsberg, and J. E. Darnell, Jr.** 1985. Adenovirus E1B proteins are required for accumulation of late viral mRNA and for effects on cellular mRNA translation and transport. Mol. Cell. Biol. **5:**2552–2558.
2. **Bandara, L. R., E. W. F. Lam, T. S. Sorensen, M. Zamanian, R. Girling, and N. B. La Thangue.** 1994. DP-1: a cell cycle-regulated and phosphorylated component of transcription factor DRTF1/E2F which is functionally important for recognition by pRb and the adenovirus E4 orf6/7 protein. EMBO J. **13:**3104–3114.
3. **Barr, D., J. Tubb, D. Ferguson, A. Scaria, A. Lieber, C. Wilson, J. Perkins, and M. A. Kay.** 1995. Strain related variations in adenovirally mediated transgene expression from mouse hepatocytes in vivo: comparisons between immunocompetent and immunodeficient inbred strains. Gene Ther. **2:**151–155.
4. **Bondesson, M., K. Ohman, M. Mannervik, S. Fan, and G. Aküsjarvi.** 1996. Adenovirus E4 open reading frame 4 protein autoregulates E4 transcription by inhibiting E1A transactivation of the E4 promoter. J. Virol. **70:**3844–3851.
5. **Bridge, E., and G. Ketner.** 1989. Redundant control of adenovirus late gene expression by early region 4. J. Virol. **63:**631–638.
6. **Bridge, E., S. Medghalchi, S. Ubol, M. Leesong, and G. Ketner.** 1993. Adenovirus early region 4 and viral DNA synthesis. Virology **193:**794–801.
7. **Byrnes, A. P., J. E. Rusby, M. J. Wood, and H. M. Charlton.** 1995. Adenovirus gene transfer causes inflammation in the brain. Neurosciences **66:**1015–1024.
8. **Chang, L.-S., and T. Shenk.** 1990. The adenovirus DNA-binding protein stimulates the rate of transcription directed by adenovirus and adeno-associated virus promoters. J. Virol. **64:**2103–2109.
9. **Cohen-Tannoudji, M., D. Morello, and C. Babinet.** 1992. Unexpected position-dependent expression of H-2 and β2-microglobulin/lacZ transgenes. Mol. Reprod. Dev. **33:**149–159.
10. **Daï, Y., H. M. Schwarz, D. Gu, W.-W. Zhang, N. Sarvetnick, and I. M. Verma.** 1995. Cellular and humoral immune responses to adenoviral vectors containing factor IX gene: tolerization of factor IX and vector antigens allows for long-term expression. Proc. Natl. Acad. Sci. USA **92:**1401–1405.
11. **Dedieu, J.-F.** Unpublished data.
12. **Dix, I., and K. N. Leppard.** 1993. Regulated splicing of adenovirus type 5 E4 transcripts and regulated cytoplasmic accumulation of E4 mRNA. J. Virol. **67:**3226–3231.
13. **Dobner, T., N. Horikoshi, S. Rubenwolf, and T. Shenk.** 1996. Blockage by adenovirus E4orf6 of transcriptional activation by the p53 tumor suppressor. Science **272:**1470–1473.
14. **Engelhardt, J. F., Y. Yang, L. D. Stratford-Perricaudet, E. D. Allen, K. Kozarsky, M. Perricaudet, J. R. Yankaskas, and J. M. Wilson.** 1993. Direct gene transfer of human CFTR into human bronchial epithelia of xenografts with E1-deleted adenovirus. Nat. Genet. **4:**27–34.
15. **Fagan, R., K. J. Flint, and N. Jones.** 1994. Phosphorylation of E2F-1 modulates its interaction with the retinoblastoma gene product and the adenoviral E4 19 kDa protein. Cell **78:**799–811.
16. **Falgout, B., and G. Ketner.** 1987. Adenovirus early region 4 is required for efficient virus particle assembly. J. Virol. **61:**3759–3768.
17. **Farrell Jr, R. E.** 1993. RNA methodologies: a laboratory guide for isolation and characterisation. Academic Press, London, United Kingdom.
18. **Gao, G.-P., Y. Yang, and J. M. Wilson.** 1996. Biology of adenovirus vectors with E1 and E4 deletions for liver-directed gene therapy. J. Virol. **70:**8934–8943.
19. **Ginsberg, H. S., L. L. Moldawer, P. B. Sehgal, M. Redington, P. L. Kilian, R. M. Chanock, and G. A. Prince.** 1991. A mouse model for investigating the molecular pathogenesis of adenovirus pneumonia. Proc. Natl. Acad. Sci. USA **88:**1651–1655.
20. **Goodrum, F. D., T. Shenk, and D. A. Ornelles.** 1996. Adenovirus early region 4 34-kilodalton protein directs the nuclear localization of the early region 1B 55-kilodalton protein in primate cells. J. Virol. **70:**6323–6335.
21. **Gorziglia, M. I., M. J. Kadan, S. Yei, J. Lim, G. M. Lee, R. Luthra, and B. C. Trapnell.** 1996. Elimination of both E1 and E2a from adenovirus vectors

further improves prospects for in vivo human gene therapy. J. Virol. **70:** 4173–4178.
22. **Graham, F. L., J. Smiley, W. C. Russel, and R. Nairn.** 1977. Characteristics of a human cell line transformed by DNA from human adenovirus type 5. J. Gen. Virol. **36:**59–72.
23. **Halbert, D. N., J. R. Cutt, and T. Shenk.** 1985. Adenovirus early region 4 encodes functions required for efficient DNA replication, late gene expression, and host cell shutoff. J. Virol. **56:**250–257.
24. **Helin, K., and E. Harlow.** 1994. Heterodimerization of the transcription factors E2F-1 and DP-1 is required for binding to the adenovirus E4 (ORF6/7) protein. J. Virol. **68:**5027–5035.
25. **Hemstrom, C., K. Nordqvist, U. Pettersson, and A. Virtanen.** 1988. Gene product of region E4 of adenovirus type 5 modulates accumulation of certain viral polypeptides. J. Virol. **62:**3258–3264.
26. **Hirt, B.** 1967. Selective extraction of polyoma DNA from infected mouse cell cultures. J. Mol. Biol. **26:**365–369.
27. **Huang, M. M., and P. Hearing.** 1989. Adenovirus early region 4 encodes two gene products with redundant effects in lytic infection. J. Virol. **63:**2605–2615.
28. **Kleinberger, T., and T. Shenk.** 1993. Adenovirus E4orf4 protein binds to protein phosphatase 2A, and the complex down regulates E1A-enhanced *junB* transcription. J. Virol. **67:**7556–7560.
29. **Kozarsky, K. F., D. R. McKinley, L. L. Austin, S. E. Raper, L. D. Stratford-Perricaudet, and J. M. Wilson.** 1994. In vivo correction of low density lipoprotein receptor deficiency in the Watanabe heritable hyperlipidemic rabbit with recombinant adenoviruses. J. Biol. Chem. **269:**13695–13702.
30. **Krougliak, V., and F. L. Graham.** 1995. Development of cell lines capable of complementing E1, E4, and protein IX defective adenovirus type 5 mutants. Hum. Gene Ther. **6:**1575–1586.
31. **Lang, A., V. J. Fincham, and J. A. Wyke.** 1993. Factors influencing physiological variations in the activity of the Rous sarcoma virus long terminal repeat. Virology **196:**564–575.
32. **Leader, D. P., I. Gall, P. Campbell, and A. M. Frischauf.** 1986. Isolation and characterisation of cDNA clones from mouse skeletal actin mRNA. DNA **5:**235–238.
33. **Malone, R. W., M. A. Hickman, K. Lehmann-Bruinsma, T. R. Sih, R. Walzem, D. M. Carlson, and J. S. Powell.** 1994. Dexamethasone enhancement of gene expression after direct hepatic DNA injection. J. Biol. Chem. **269:** 29903–29907.
34. **Moore, M., N. Horikoshi, and T. Shenk.** 1996. Oncogenic potential of the adenovirus E4orf6 protein. Proc. Natl. Acad. Sci. USA **93:**11295–11301.
35. **Müller, U., T. Kleinberger, and T. Shenk.** 1992. Adenovirus E4Orf4 protein reduces phosphorylation of c-Fos and E1A proteins while simultaneously reducing the level of AP1. J. Virol. **66:**5867–5878.
36. **Nordqvist, K., K. Ohman, and G. Aküsjarvi.** 1994. Human adenovirus encodes two proteins which have opposite effects on accumulation of alternatively spliced mRNAs. Mol. Cell. Biol. **14:**437–445.
37. **O'Connor, R. J., and P. Hearing.** 1994. Mutually exclusive interaction of the adenovirus E4-6/7 protein and the retinoblastoma gene product with internal domains of E2F-1 and DP-1. J. Virol. **68:**6848–6862.
38. **Overbeek, P. A., S.-P. Lai, R. V. Van Quill, and H. Westphal.** 1986. Tissue-specific expression in transgenic mice of a fused gene containing RSV terminal sequences. Science **231:**1574–1577.
39. **Parker Ponder, K., R. P. Dunbar, D. R. Wilson, G. J. Darlington, and S. L. C. Woo.** 1991. Evaluation of relative promoter strength in primary hepatocytes using optimized lipofection. Hum. Gene Ther. **2:**41–52.
40. **Pilder, S., M. Moore, J. Logan, and T. Shenk.** 1986. The adenovirus E1B-55K transforming polypeptide modulates transport or cytoplasmic stabilization of viral and host cell mRNAs. Mol. Cell. Biol. **6:**470–476.
41. **Ryden, T. A., M. de Mars, and K. Beemon.** 1993. Mutation of the C/EBP binding sites in the Rous sarcoma virus long terminal repeat and *gag* enhancers. J. Virol. **67:**2862–2870.
42. **Sandler, A. B., and G. Ketner.** 1991. The metabolism of host RNAs in cells infected by an adenovirus E4 mutant. Virology **181:**319–326.
43. **Sarnow, P., P. Hearing, C. W. Anderson, D. N. Halbert, T. Shenk, and A. J. Levine.** 1984. Adenovirus early region 1B 58,000-dalton tumor antigen is physically associated with an early region 4 25,000-dalton protein in productively infected cells. J. Virol. **49:**692–700.
44. **Schaack, J., H. F. Maguire, and A. Siddiqui.** 1996. Hepatitis B virus X protein partially substitutes for E1A transcriptional function during adenovirus infection. Virology **216:**425–430.
45. **Shenk, T.** 1996. Adenoviridae: the viruses and their replication, p. 2111–2148. *In* B. N. Fields, D. M. Knipe, P. M. Howley, et al. (ed.) Virology. Raven Press, Philadelphia, Pa.
46. **Spergel, J. M., W. Hsu, S. Akira, B. Thimmappaya, T. Kishimoto, and S. Chen-Kiang.** 1992. NF-IL6, a member of the C/EBP family, regulates E1A-responsive promoters in the absence of E1A. J. Virol. **66:**1021–1030.
47. **Stallcup, M. R., and L. D. Washington.** 1983. Region-specific initiation of mouse mammary tumor virus RNA synthesis by endogenous RNA polymerase II in preparations of cell nuclei. J. Biol. Chem. **258:**2802–2809.
48. **Stratford-Perricaudet, L. D., I. Makeh, M. Perricaudet, and P. Briand.** 1992. Widespread long-term gene transfer to mouse skeletal muscles and heart via an adenovirus vector. J. Clin. Invest. **90:**626–630.
49. **Tripathy, S. K., H. B. Black, E. Goldwasser, and J. M. Leiden.** 1996. Immune responses to transgene-encoded proteins limit the stability of gene expression after injection of replication-defective adenovirus vectors. Nat. Med. **2:**545–550.
50. **van der Vliet, P. C.** 1990. Adenovirus DNA replication in vitro, p. 1–29. *In* P. R. Strauss and S. H. Wilson (ed.), The eukaryotic nucleus, vol. 1. Telford Press, Caldwell, N.J.
51. **Varley, A. W., M. G. Coulthard, R. S. Meidell, R. D. Gerard, and R. S. Munford.** 1995. Inflammation-induced recombinant protein expression in vivo using promoters from acute-phase protein genes. Proc. Natl. Acad. Sci. USA **92:**5346–5350.
52. **Vigne, E.** Unpublished data.
53. **Wang, Q., and M. H. Finer.** 1995. A packaging cell line for propagation of recombinant adenovirus vector containing two lethal gene-region deletions. Gene Ther. **2:**775–783.
54. **Weiden, M. D., and H. S. Ginsberg.** 1994. Deletion of the E4 region of the genome produces adenovirus DNA concatemers. Proc. Natl. Acad. Sci. USA **91:**153–157.
55. **Weinberg, D. H., and G. Ketner.** 1986. Adenoviral early region 4 is required for efficient viral DNA replication and for late gene expression. J. Virol. **57:**833–838.
56. **Weinberg, D. H., and G. Ketner.** 1983. A cell line that supports the growth of a defective early region 4 deletion mutant of human adenovirus type 2. Proc. Natl. Acad. Sci. USA **80:**5383–5386.
57. **Yang, Y., H. C. J. Ertl, and J. M. Wilson.** 1994. MHC class I-restricted cytotoxic T lymphocytes to viral antigens destroy hepatocytes in mice infected with E1-deleted recombinant adenoviruses. Immunity **1:**433–442.
58. **Yang, Y., K. U. Jooss, Q. Su, H. C. Ertl, and J. M. Wilson.** 1996. Immune responses to viral antigens versus transgene product in the elimination of recombinant adenovirus-infected hepatocytes in vivo. Gene Ther. **3:**137–144.
59. **Yang, Y., F. A. Nunes, K. Berencsi, E. E. Furth, E. Gonczol, and J. M. Wilson.** 1994. Cellular immunity to viral antigens limits E1-deleted adenoviruses for gene therapy. Proc. Natl. Acad. Sci. USA **91:**4407–4411.
60. **Yeh, P., J.-F. Dedieu, C. Orsini, E. Vigne, P. Denèfle, and M. Perricaudet.** 1996. Efficient dual transcomplementation of adenovirus E1 and E4 regions from a 293-derived cell line expressing a minimal E4 functional unit. J. Virol. **70:**559–565.
61. **Zambetti, G. P., and A. J. Levine.** 1993. A comparison of the biological activities of wild-type and mutant p53. FASEB J. **7:**855–865.
62. **Zijderveld, D. C., F. d'Adda di Fagagna, M. Giacca, H. T. Marc Timmers, and P. van der Vliet.** 1994. Stimulation of the adenovirus major late promoter in vitro by transcription factor USF is enhanced by the adenovirus DNA binding protein. J. Virol. **68:**8288–8295.